The design of random surfaces that produce nonstandard refraction of light

T. A. Leskova[a], A. A. Maradudin[a], and I. Simonsen[b]

[a] Department of Physics and Astronomy
and Institute for Surface and Interface Science
University of California, Irvine CA 92697, U.S.A.
[b] Department of Physics, Norwegian University of Science and Technology (NTNU),
NO-7491, Trondheim, Norway

ABSTRACT

On the basis of the geometrical optics limit of the Kirchhoff approximation we design a one-dimensional random interface between two dielectric media that refracts $p-$ or $s-$polarized light incident on it at an arbitrary angle of incidence θ_0 from one of them into the other at an arbitrary but specified angle of transmission θ_t that is not defined in terms of θ_0 by Snell's law. We call such transmission *nonstandard refraction*.

1. INTRODUCTION

In recent theoretical studies it has been shown how to design one-dimensional randomly rough surfaces that transmit an electromagnetic wave with a prescribed angular dependence of the mean differential transmission coefficient.[1,2] The results of these studies suggest that it should be possible to design a one-dimensional randomly rough interface that refracts light falling on it at a given angle of incidence θ_0 from a dielectric medium characterized by a dielectric constant ϵ_1 through an arbitrary but specified angle θ_t in a dielectric medium with a dielectric constant ϵ_2. We will call this type of refraction *nonstandard refraction* because it is free from the constraint of Snell's law $\sin\theta_t/\sin\theta_0 = \sqrt{\epsilon_1/\epsilon_2}$. It encompasses negative refraction,[3] for example.

In this paper we show that it is indeed possible to design a one-dimensional randomly rough surface that produces nonstandard refraction. Our theoretical treatment, however, is more general than its application to nonstandard refraction, and the results obtained here could be useful for the solution of other problems involving the transmission of light through a randomly rough interface.

The results of our investigations are validated by rigorous computer simulation calculations of the transmission of light from the surfaces designed by the approach presented here.

2. SCATTERING THEORY

The scattering system we consider in this work consists of a dielectric medium whose dielectric constant is ϵ_1 in the region $x_3 > \zeta(x_1)$, and a dielectric medium whose dielectric constant is ϵ_2 in the region $x_3 < \zeta(x_1)$. We assume that ϵ_1 and ϵ_2 are both real, positive, and frequency independent. The surface profile function $\zeta(x_1)$ is a single-valued function of x_1 and constitutes a random process, but not necessarily a stationary one. The surface $x_3 = \zeta(x_1)$ is illuminated from the region $x_3 > \zeta(x_1)$ by a $p-$ or $s-$polarized plane wave of frequency ω, whose plane of incidence is the x_1x_3 plane. There is no cross-polarized scattering in this geometry.

We can deal with the cases of p- and s-polarized incident light simultaneously by working with the function $F_\nu(x_1, x_3|\omega)$, which is $H_2(x_1, x_2|\omega)$ when $\nu = p$, and is $E_2(x_1, x_3|\omega)$ when $\nu = s$. Here $H_2(x_1, x_3|\omega)$ $(E_2(x_1, x_3|\omega))$ is the single nonzero component of the magnetic (electric) field in the system in the case of $p(s)$ polarization.

The field $F_\nu^>(x_1, x_3|\omega)$ in the region $x_3 > \zeta(x_1)$ satisfies the Helmholtz equation

$$\left(\frac{\partial^2}{\partial x_1^2} + \frac{\partial^2}{\partial x_3^2} + \epsilon_1\frac{\omega^2}{c^2}\right) F_\nu^>(x_1, x_3|\omega) = 0. \tag{2.1}$$

Reflection, Scattering, and Diffraction from Surfaces, edited by Zu-Han Gu,
Leonard M. Hanssen, Proc. of SPIE Vol. 7065, 706506, (2008)
0277-786X/08/$18 · doi: 10.1117/12.796093

The field $F_\nu^<(x_1,x_3|\omega)$ in the region $x_3<\zeta(x_1)$ satisfies the Helmholtz equation

$$\left(\frac{\partial^2}{\partial x_1^2}+\frac{\partial^2}{\partial x_3^2}+\epsilon_2\frac{\omega^2}{c^2}\right)F_\nu^<(x_1,x_3|\omega)=0. \tag{2.2}$$

The boundary conditions at the interface $x_3=\zeta(x_1)$ require the continuity of the tangential components of the electric and magnetic fields across it, and can be written as

$$F_\nu^>(x_1,x_3|\omega)\Big|_{x_3=\zeta(x_1)} = F_\nu^<(x_1,x_3|\omega)\Big|_{x_3=\zeta(x_1)} \tag{2.3a}$$

$$\frac{1}{\kappa_\nu}\frac{\partial}{\partial n}F_\nu^>(x_1,x_3|\omega)\Big|_{x_3=\zeta(x_1)} = \frac{1}{\mu_\nu}\frac{\partial}{\partial n}F_\nu^<(x_1,x_3|\omega)\Big|_{x_3=\zeta(x_1)}. \tag{2.3b}$$

In these equations $\kappa_p=\epsilon_1,\kappa_s=1$, and $\mu_p=\epsilon_2,\mu_s=1$, and $\partial/\partial n$ is the derivative along the normal to the surface $x_3=\zeta(x_1)$ at each point of it directed from medium 2 into medium 1,

$$\frac{\partial}{\partial n}=\frac{1}{[1+(\zeta'(x_1))^2]^{\frac{1}{2}}}\left(-\zeta'(x_1)\frac{\partial}{\partial x_1}+\frac{\partial}{\partial x_3}\right). \tag{2.4}$$

In addition, $F_\nu^>(x_1,x_3|\omega)$ consists of an incoming incident plane wave and outgoing scattered waves at $x_3=\infty$, and $F_\nu^<(x_1,x_3|\omega)$ consists of outgoing transmitted waves at $x_3=-\infty$.

We next introduce two Green's functions $G_j(x_1,x_3|x_1',x_3')$ $(j=1,2)$ that satisfy the equations

$$\left(\frac{\partial^2}{\partial x_1^2}+\frac{\partial^2}{\partial x_3^2}+\epsilon_j\frac{\omega^2}{c^2}\right)G_j(x_1,x_3|x_1',x_3')=-4\pi\delta(x_1-x_1')\delta(x_3-x_3') \tag{2.5}$$

in all space, subject to outgoing wave boundary conditions at infinity. These functions have the representations

$$G_j(x_1,x_3|x_1',x_3') = i\pi H_0^{(1)}(n_j(\omega/c)[(x_1-x_1')^2+(x_3-x_3')^2]^{\frac{1}{2}}) \tag{2.6a}$$

$$= \int_{-\infty}^{\infty}\frac{dq}{2\pi}\frac{2\pi i}{\alpha_j(q)}\exp[iq(x_1-x_1')+i\alpha_j(q)|x_3-x_3'|], \tag{2.6b}$$

where $H_0^{(1)}(z)$ is a Hankel function of the first kind and zero order, n_j is the index of refraction of medium j, $n_j=(\epsilon_j)^{\frac{1}{2}}$, and

$$\alpha_j(q)=[\epsilon_j(\omega/c)^2-q^2]^{\frac{1}{2}} \qquad Re\alpha_j(q)>0, \quad Im\alpha_j(q)>0. \tag{2.7}$$

We now invoke Green's second integral identity in the plane,[4] which applies to a bounded, planar, singly-connected region R of the x_1x_3 plane, whose boundary is a closed regular curve C. Thus, let $u(x_1,x_3)$ and $v(x_1,x_3)$ be two arbitrary functions of x_1 and x_3, which together with their first partial derivatives are continuous in the region R and on the curve C. The theorem states that

$$\int_R\int dx_1dx_3(u\nabla^2v-v\nabla^2u)=\int_C ds\left(u\frac{\partial v}{\partial\nu}-v\frac{\partial u}{\partial\nu}\right), \tag{2.8}$$

where $\nabla^2=(\partial^2/\partial x_1^2+\partial^2/\partial x_3^2)$, ds is the element of arc length along the curve C, and $\partial/\partial\nu$ is the derivative along the curve C at each point of it, directed away from the region R.

We apply Green's second integral identity in the plane, Eq. (2.8), to the region $x_3<\zeta(x_1)$. In this region we set $u(x_1,x_3)=F_\nu^<(x_1,x_3|\omega)$ and $v(x_1,x_3)=G_2(x_1,x_3|x_1',x_3')$. For the curve C we take the union of the curve

$x_3 = \zeta(x_1)$, which we denote by s, and a semicircle of infinite radius in the region $x_3 < \zeta(x_1)$, which we denote by $C^{(-\infty)}$. Because the transmitted field satisfies a radiation condition at infinity, and there is no incident field in the region $x_3 < \zeta(x_1)$, the integral along the semicircle $C^{(-\infty)}$ vanishes. The equation for $F_\nu^<(x_1, x_3|\omega)$ can therefore be rewritten as

$$\theta(\zeta(x_1) - x_3)F_\nu^<(x_1, x_3|\omega) = -\frac{1}{4\pi}\int_s ds' \left[\left(\frac{\partial}{\partial n'}G_2(x_1, x_3|x_1', x_3')\right) F_\nu^<(x_1', x_3'|\omega)\right.$$

$$\left. -G_2(x_1, x_3|x_1', x_3')\frac{\partial}{\partial n'}F_\nu^<(x_1', x_3'|\omega)\right]. \tag{2.9}$$

The field transmitted through the surface is given by the right hand side of Eq. (2.9), which we rewrite with the use of the boundary conditions (2.3) as

$$F_\nu(x_1, x_3|\omega)_{tr} = -\frac{1}{4\pi}\int_s ds' \left[\left(\frac{\partial}{\partial n'}G_2(x, x_3|x_1', x_3')\right) F_\nu^>(x_1', x_3'|\omega)\right.$$

$$\left. -\frac{\mu_\nu}{\kappa_\nu}G_2(x_1, x_3|x_1', x_3')\frac{\partial}{\partial n'}F_\nu^>(x_1', x_3'|\omega)\right]. \tag{2.10}$$

With the use of the representation (2.6b) for the Green's function $G_2(x_1, x_3|x_1', x_3')$ the transmitted field in the case that $|x_3| \gg |x_3'|$ can be written as

$$F_\nu(x_1, x_3|\omega)_{tr} = \int_{-\infty}^{\infty}\frac{dq}{2\pi}T_\nu(q|k)\exp[iqx_1 - i\alpha_2(q)x_3], \tag{2.11}$$

where the transmission amplitude $T_\nu(q|k)$ is

$$T_\nu(q|k) = -\frac{i}{2\alpha_2(q)}\int_s ds \exp[-iqx_1 + i\alpha_2(q)x_3]$$

$$\times\left\{\frac{i[q\zeta'(x_1) + \alpha_2(q)]}{[1 + (\zeta'(x_1))^2]^{\frac{1}{2}}}F_\nu^>(x_1, x_3|\omega) - \frac{\mu_\nu}{\kappa_\nu}\frac{\partial}{\partial n}F_\nu^>(x_1, x_3|\omega)\right\}. \tag{2.12}$$

The dependence of the transmission amplitude on a wavenumber k arises from the dependence on this wavenumber of the incident field, which we write in the form

$$F_\nu(x_1, x_3|\omega)_{inc} = \exp[ikx_1 - i\alpha_1(k)x_3]. \tag{2.13}$$

3. THE MEAN DIFFERENTIAL TRANSMISSION COEFFICIENT

The transmission amplitude $T_\nu(q|k)$ plays a central role in the present work, because the mean differential transmission coefficient is expressed in terms of this amplitude. The differential transmission coefficient $(\partial T_\nu/\partial\theta_t)$ is defined such that $(\partial T_\nu/\partial\theta_t))d\theta_t$ is the fraction of the total time-averaged incident flux that is transmitted into the angular interval $(\theta_t, \theta_t + d\theta_t)$ about the direction of transmission defined by the angle of transmission θ_t.

The real part of the 3-component of the complex Poynting vector in the region $x_3 > \zeta(x_1)$ is

$$Re\,(S_3^c)_\nu = Re\left(-i\frac{c^2}{8\pi\omega\kappa_\nu}\frac{\partial F_\nu}{\partial x_3}F_\nu^*\right). \tag{3.1}$$

When the incident field is a plane wave, Eq. (2.13), the magnitude of the time-averaged flux incident on the region $|x_1| < L_1/2, |x_2| < L_2/2$ of the plane $x_3 = 0$ is

$$\begin{aligned}(P_{inc})_\nu &= -\int_{-\frac{L_1}{2}}^{\frac{L_1}{2}} dx_1 \int_{-\frac{L_2}{2}}^{\frac{L_2}{2}} dx_2 Re\left[-i\frac{c^2}{8\pi\omega\kappa_\nu}(-i\alpha_1(k))\right] \\ &= L_1 L_2 \frac{c^2\alpha_1(k)}{8\pi\omega\kappa_\nu}. \end{aligned} \tag{3.2}$$

The minus sign in front of the integral on the right-hand side of Eq. (3.2) compensates for the fact that the 3-component of the Poynting vector of the incident field is negative.

We introduce the angle of incidence θ_0, measured counterclockwise from the x_3 axis, by

$$k = \sqrt{\epsilon_1}(\omega/c)\sin\theta_0. \tag{3.3}$$

The total time-averaged incident flux then becomes

$$(P_{inc}(\theta_0))_\nu = L_1 L_2 \frac{c}{8\pi}\frac{\sqrt{\epsilon_1}}{\kappa_\nu}\cos\theta_0. \tag{3.4}$$

The real part of the 3-component of the complex Poynting vector in the region $x_3 < \zeta(x_1)$ is

$$Re(S_3^c)_\nu = Re\left(-i\frac{c^2}{8\pi\omega\mu_\nu}\frac{\partial F_\nu}{\partial x_3}F_\nu^*\right). \tag{3.5}$$

The transmitted field in the region $x_3 < \zeta(x_1)$ is given by Eq. (2.11). The magnitude of the total time-averaged flux transmitted through the region $|x_1| < L_1/2, |x_2| < L_2/2$ of the plane $x_3 = 0$ is given by

$$\begin{aligned}(P_{tr})_\nu &= -\int_{-\frac{L_1}{2}}^{\frac{L_1}{2}} dx_1 \int_{-\frac{L_2}{2}}^{\frac{L_2}{2}} dx_2 Re\left(-i\frac{c^2}{8\pi\omega\mu_\nu}\right)\int_{-\infty}^{\infty}\frac{dq}{2\pi}\int_{-\infty}^{\infty}\frac{dq'}{2\pi} \\ &\quad \times(-i\alpha_2(q))T_\nu(q|k)T_\nu^*(q'|k)\exp[-i(q-q')x_1]\exp[-i(\alpha_2(q)-\alpha_2^*(q'))x_3] \\ &= L_2\frac{c^2}{16\pi^2\omega\mu_\nu}\int_{-\sqrt{\epsilon_2}(\omega/c)}^{\sqrt{\epsilon_2}(\omega/c)} dq\,\alpha_2(q)|T_\nu(q|k)|^2, \end{aligned} \tag{3.6}$$

when we let L_1 tend to infinity. Again, the minus sign in front of the integral on the right-hand side of Eq. (3.6) compensates for the fact that the 3-component of the Poynting vector of the transmitted field is negative.

We now introduce the angle of transmission θ_t, measured counterclockwise from the negative x_3 axis by

$$q = \sqrt{\epsilon_2}(\omega/c)\sin\theta_t. \tag{3.7}$$

The total time-averaged transmitted flux then takes the form

$$(P_{tr})_\nu = \int_{-\frac{\pi}{2}}^{\frac{\pi}{2}} d\theta_t (P_{tr}(\theta_t))_\nu, \tag{3.8}$$

where

$$(P_{tr}(\theta_t))_\nu = L_2 \frac{\omega\epsilon_2}{16\pi^2\mu_\nu} \cos^2\theta_t |T_\nu(q|k)|^2. \tag{3.9}$$

By definition the differential transmission coefficient is then given by

$$\left(\frac{\partial T_\nu}{\partial\theta_t}\right)(\theta_t,\theta_0) = \frac{(P_{tr}(\theta_t))_\nu}{(P_{inc}(\theta_0))_\nu} = \frac{1}{L_1}\frac{\epsilon_2}{\sqrt{\epsilon_1}}\frac{\kappa_\nu}{\mu_\nu}\frac{\omega}{2\pi c}\frac{\cos^2\theta_t}{\cos\theta_0}|T_\nu(q|k)|^2, \tag{3.10}$$

where q and k are now given by Eqs. (3.7) and (3.3), respectively. Since we are dealing with transmission through a randomly rough surface, it is the mean differential transmission coefficient that is of interest to us, which is given by

$$\left\langle\frac{\partial T_\nu}{\partial\theta_t}\right\rangle(\theta_t,\theta_0) = \frac{1}{L_1}\frac{\epsilon_2}{\sqrt{\epsilon_1}}\frac{\kappa_\nu}{\mu_\nu}\frac{\omega}{2\pi c}\frac{\cos^2\theta_t}{\cos\theta_0}\langle|T_\nu(q|k)|^2\rangle. \tag{3.11}$$

4. THE KIRCHHOFF APPROXIMATION

The transmission amplitude $T_\nu(q|k)$, Eq. (2.12), needs to be known analytically if we are to be able to solve the inverse problem of finding a surface profile function $\zeta(x_1)$ that produces a mean differential transmission coefficient with a specified dependence on θ_t for a given value of θ_0. The Kirchhoff approximation[5] provides such a result, and we use it in this work. By applying the approach of Voronovich[5] to the problem of of transmission through a one-dimensional rough surface we find that the transmission amplitude is given by

$$T_\nu(q|k) = T_\nu^{(0)}(q|k)\int_{-\infty}^{\infty} dx_1 \exp\{-i(q-k)x_1 + i[\alpha_2(q)-\alpha_1(k)]\zeta(x_1)\}, \tag{4.1a}$$

where

$$\begin{aligned} T_\nu^{(0)}(q|k) &= \frac{1}{2\alpha_2(q)}\frac{1}{\alpha_2(q)-\alpha_1(k)}\left\{\left[\left(\epsilon_2 - \frac{\mu_\nu}{\kappa_\nu}\epsilon_1\right)\frac{\omega^2}{c^2} - \left(1-\frac{\mu_\nu}{\kappa_\nu}\right)(qk+\alpha_2(q)\alpha_1(k))\right]\right. \\ &\quad \left. + \left[\left(\epsilon_2 + \frac{\mu_\nu}{\kappa_\nu}\epsilon_1\right)\frac{\omega^2}{c^2} - \left(1+\frac{\mu_\nu}{\kappa_\nu}\right)(qk+\alpha_2(q)\alpha_1(k))\right]R_\nu(\alpha_\ell(k|x_{1i})\right\}, \end{aligned} \tag{4.1b}$$

and $R_\nu(\alpha_\ell(k|x_{1i}))$ is the Fresnel reflection amplitude evaluated at the local angle of incidence, i.e. the angle of incidence measured from the normal to the surface at each point,

$$R_\nu(\alpha_\ell(k|x_{i\ell})) = \frac{\mu_\nu\alpha_\ell(k|x_{1i}) - \kappa_\nu[(\epsilon_2-\epsilon_1)(\omega/c)^2 + \alpha_\ell^2(k|x_{1i})]^{\frac{1}{2}}}{\mu_\nu\alpha_\ell(k|x_{1i}) + \kappa_\nu[(\epsilon_2-\epsilon_1)(\omega/c)^2 + \alpha_\ell^2(k|x_{1i}))]^{\frac{1}{2}}}, \tag{4.2a}$$

with

$$\alpha_\ell(k|x_{1i}) = \frac{|\alpha_2(q)-\alpha_1(k)|}{\alpha_2(q)-\alpha_1(k)}\frac{\alpha_2(q)\alpha_1(k)+qk-\epsilon_1(\omega/c)^2}{\sqrt{2}[\frac{1}{2}(\epsilon_1+\epsilon_2)(\omega/c)^2 - \alpha_2(q)\alpha_1(k) - qk]^{\frac{1}{2}}}. \tag{4.2b}$$

Equation (4.1) is the tangent plane or Kirchhoff approximation to the transmission amplitude $T_\nu(q|k)$.

The expression for $T_\nu^{(0)}(q|k)$ can be rewritten in terms of the angles θ_0 and θ_t, through the use of Eqs. (3.3) and (3.7) together with Eqs. (4.2). The result is

$$\begin{aligned} T_\nu^{(0)}(q|k) &= \frac{\mu_\nu\sqrt{\epsilon_1}}{\cos\theta_t}\frac{\sqrt{\epsilon_2}\cos(\theta_t-\theta_0)-\sqrt{\epsilon_1}}{\sqrt{\epsilon_2}\cos\theta_t-\sqrt{\epsilon_1}\cos\theta_0} \\ &\quad\times\frac{s[\sqrt{\epsilon_2}-\sqrt{\epsilon_1}\cos(\theta_t-\theta_0)]+|\sqrt{\epsilon_2}-\sqrt{\epsilon_1}\cos(\theta_t-\theta_0)|}{s\mu_\nu\sqrt{\epsilon_1}[\sqrt{\epsilon_2}\cos(\theta_t-\theta_0)-\sqrt{\epsilon_1}]+\kappa_\nu\sqrt{\epsilon_2}|\sqrt{\epsilon_1}\cos(\theta_t-\theta_0)-\sqrt{\epsilon_2}|} \\ &\equiv t_\nu^{(0)}(\theta_t|\theta_0), \end{aligned} \tag{4.3}$$

where

$$s \equiv sgn(\sqrt{\epsilon_2}\cos\theta_t-\sqrt{\epsilon_1}\cos\theta_0). \tag{4.4}$$

5. THE INVERSE PROBLEM

The results obtained in the preceding sections enable us now to solve the inverse problem of determining the surface profile function $\zeta(x_1)$ that gives rise to a transmitted field with a specified mean differential transmission coefficient $\langle\partial T_\nu/\partial\theta_t\rangle(\theta_t,\theta_0)$.

The mean differential transmission coefficient in the Kirchhoff approximation is obtained from Eqs. (3.11), (4.1a), and (4.3) in the form

$$\begin{aligned} \left\langle\frac{\partial T_\nu}{\partial\theta_t}\right\rangle(\theta_t,\theta_0) &= \frac{1}{L_1}\frac{\epsilon_2}{\sqrt{\epsilon_1}}\frac{\kappa_\nu}{\mu_\nu}\frac{\omega}{2\pi c}\frac{\cos^2\theta_t}{\cos\theta_0}|t_\nu^{(0)}(\theta_t|\theta_0)|^2 \\ &\quad\times\int_{-\infty}^{\infty}dx_1\int_{-\infty}^{\infty}dx_1'\exp[-i(q-k)(x_1-x_1')]\langle\exp\{i[\alpha_2(q)-\alpha_1(k)][\zeta(x_1)-\zeta(x_1')]\}\rangle. \end{aligned} \tag{5.1}$$

As it stands, Eq. (5.1) is too complicated to invert to obtain $\zeta(x_1)$ in terms of $\langle\partial T_\nu/\partial\theta_t\rangle(\theta_t,\theta_0)$. To obtain an expression that can be inverted, we pass to the geometrical optics limit of Eq. (5.1). This is done by expanding $\zeta(x_1)$ about x_1',

$$\zeta(x_1) = \zeta(x_1') + (x_1-x_1')\zeta'(x_1') + \cdots, \tag{5.2}$$

and retaining only the first two terms in this expansion. In this way we obtain the result

$$\begin{aligned} \left\langle\frac{\partial T_\nu}{\partial\theta_t}\right\rangle(\theta_t,\theta_0) &= \frac{1}{L_1}\frac{\epsilon_2}{\sqrt{\epsilon_1}}\frac{\kappa_\nu}{\mu_\nu}\frac{\omega}{2\pi c}\frac{\cos^2\theta_t}{\cos\theta_0}|t_\nu^{(0)}(\theta_t|\theta_0)|^2 \\ &\quad\times\int_{-\infty}^{\infty}dx_1\int_{-\infty}^{\infty}dx_1'\exp[-i(q-k)(x_1-x_1')]\langle\exp\{i[\alpha_2(q)-\alpha_1(k)](x_1-x_1')\zeta'(x_1')\}\rangle. \end{aligned} \tag{5.3}$$

To evaluate the double integral in Eq. (5.3) we recall that we assumed that the surface profile function $\zeta(x_1)$ is nonzero only for x_1 within an interval of length L_1 of the x_1 axis. Within this interval we represent $\zeta(x_1)$ in the form

$$\zeta(x_1) = a_n(x_1-nb), \qquad nb < x_1 < (n+1)b, \qquad n = -N, -N=1,\ldots,N-1, \tag{5.4}$$

where $\{a_n\}$ are independent, identically distributed random deviates, b is a characteristic length, and N is a large positive integer. The length L_1 is therefore $L_1 = 2Nb$. Because the $\{a_n\}$ are independent and identically distributed random deviates, the probability density function (pdf) of a_n,

$$f(\gamma) = \langle \delta(\gamma - a_n) \rangle, \tag{5.5}$$

is independent of n.

With the definition $a(q,k) = \alpha_2(q) - \alpha_1(k)$ the double integral in Eq. (5.3) can be evaluated as

$$I = 4(Nb)^2 \int_{-\infty}^{\infty} d\gamma f(\gamma) [\mathrm{sinc}(q - k - a\gamma)Nb]^2, \tag{5.6}$$

where $\mathrm{sinc}x = sinx/x$. In the limit as $N \to \infty$ we have

$$(\mathrm{sinc}Nx)^2 \to \frac{\pi}{N}\delta(x). \tag{5.7}$$

It follows, then, that Eq. (5.6) becomes

$$\begin{aligned} I &= \frac{4\pi Nb}{|a|} f\left(\frac{q-k}{a}\right) \\ &= \frac{2\pi L_1}{|\alpha_2(q) - \alpha_1(k)|} f\left(\frac{q-k}{\alpha_2(q) - \alpha_1(k)}\right). \end{aligned} \tag{5.8}$$

When this result is substituted into Eq.(5.3), and use is made of Eqs. (3.3) and (3.7), we obtain the mean differential transmission coefficient in the form

$$\left\langle \frac{\partial T_\nu}{\partial \theta_t} \right\rangle (\theta_t, \theta_0) = \frac{\epsilon_2}{\sqrt{\epsilon_1}} \frac{\kappa_\nu}{\mu_\nu} \frac{\cos^2\theta_t}{\cos\theta_0} \frac{|t_\nu^{(0)}(\theta_t|\theta_0)|^2}{|\sqrt{\epsilon_2}\cos\theta_t - \sqrt{\epsilon_1}\cos\theta_0|} f_\nu \left(\frac{\sqrt{\epsilon_2}\sin\theta_t - \sqrt{\epsilon_1}\sin\theta_0}{\sqrt{\epsilon_2}\cos\theta_t - \sqrt{\epsilon_1}\cos\theta_0} \right). \tag{5.9}$$

The addition of the subscript to $f(\gamma)$ emphasizes the result that the surface profile now depends on the polarization of the incident light. We now make the change of variable

$$\frac{\sqrt{\epsilon_2}\sin\theta_t - \sqrt{\epsilon_1}\sin\theta_0}{\sqrt{\epsilon_2}\cos\theta_t - \sqrt{\epsilon_1}\cos\theta_0} = -\gamma, \tag{5.10}$$

and obtain the results

$$\cos\theta_t = \sqrt{\frac{\epsilon_1}{\epsilon_2}} \frac{(\sin\theta_0 + \gamma\cos\theta_0)\gamma}{1+\gamma^2} + \frac{A(\gamma,\theta_0)}{1+\gamma^2} \tag{5.11}$$

$$\sin\theta_t = \sqrt{\frac{\epsilon_1}{\epsilon_2}} \frac{\sin\theta_0 + \gamma\cos\theta_0}{1+\gamma^2} - \frac{\gamma A(\gamma,\theta_0)}{1+\gamma^2} \tag{5.12}$$

$$\cos(\theta_t - \theta_0) = \sqrt{\frac{\epsilon_1}{\epsilon_2}} \frac{(\sin\theta_0 + \gamma\cos\theta_0)^2}{1+\gamma^2} + A(\gamma,\theta_0)\frac{\cos\theta_0 - \gamma\sin\theta_0}{1+\gamma^2}, \tag{5.13}$$

where

$$A(\gamma,\theta_0) = [1 + \gamma^2 - (\epsilon_1/\epsilon_2)(\sin\theta_0 + \gamma\cos\theta_0)^2]^{\frac{1}{2}}. \tag{5.14}$$

In what follows, to simplify the notation, we will omit the arguments of $A(\gamma,\theta_0)$ except where the result depends on the sign of γ.

In order for $\cos\theta_t$ and $\sin\theta_t$ to be real, we see that A has to be real. This requires that the inequality

$$1+\gamma^2 \geq (\epsilon_1/\epsilon_2)(\sin\theta_0+\gamma\cos\theta_0)^2 \tag{5.15}$$

be satisfied. This inequality is satisfied for all γ when $\epsilon_1 < \epsilon_2$, because $0 \leq (\sin\theta_0+\gamma\cos\theta_0)^2 \leq 1+\gamma^2$.

In the case where $\epsilon_1 > \epsilon_2$ we have to proceed carefully. It is convenient to rewrite the inequality (5.15) in the form

$$a\gamma^2 - 2b\gamma + c \geq 0, \tag{5.16}$$

where

$$a = 1-\epsilon\cos^2\theta_0 \tag{5.17a}$$

$$b = \epsilon\sin\theta_0\cos\theta_0 \tag{5.17b}$$

$$c = 1-\epsilon\sin^2\theta_0 \tag{5.17c}$$

$$\epsilon = \epsilon_1/\epsilon_2 > 1. \tag{5.17d}$$

We next write the inequality (5.16) as

$$a(\gamma-\gamma_1)(\gamma-\gamma_2) > 0. \tag{5.18}$$

where

$$\gamma_1 = \frac{b}{a} + \frac{\sqrt{\epsilon-1}}{|a|} \tag{5.19a}$$

$$\gamma_2 = \frac{b}{a} - \frac{\sqrt{\epsilon-1}}{|a|}. \tag{5.19b}$$

We see that $\gamma_1 > \gamma_2$ regardless of the signs of a and b.

We now consider the case $a > 0$, so that $\cos^2\theta_0 < 1/\epsilon$. In this case the inequality (5.18) is satisfied if

$$\gamma > \gamma_1, \qquad \gamma > \gamma_2 \tag{5.20a}$$

and if

$$\gamma < \gamma_1, \qquad \gamma < \gamma_2. \tag{5.20b}$$

Because $\gamma_1 > \gamma_2$, the pair of inequalities (5.20a) yields the constraint

$$\gamma > \gamma_1, \tag{5.21}$$

while the pair of inequalities (5.20b) yields

$$\gamma < \gamma_2. \tag{5.22}$$

Thus, when $a > 0$ A is real when $\gamma > \gamma_1$ and when $\gamma < \gamma_2$.

In the case that $a < 0$ so that $\cos^2\theta_0 > 1/\epsilon$, we see from the inequality (5.18) that it is satisfied if

$$\gamma < \gamma_1, \qquad \gamma > \gamma_2 \tag{5.23a}$$

and if

$$\gamma > \gamma_1, \qquad \gamma < \gamma_2. \tag{5.23b}$$

Since γ_1 is larger than γ_2, the second pair of inequalities cannot be satisfied simultaneously, so that the constraints on γ become

$$\gamma_2 < \gamma < \gamma_1. \tag{5.24}$$

The constraints (5.21), (5.22), and (5.24) have to be kept in mind in what follows. Their important consequence is that when they are satisfied the function A defined by Eq. (5.14) is real and positive when $\epsilon > 1$.

We now apply the preceding results to invert Eq. (5.9) to obtain $f_\nu(\gamma)$ in terms of $\langle \partial T_\nu/\partial\theta_t\rangle(\gamma,\theta_0)$, where $\langle \partial T_\nu/\partial\theta_t\rangle(\gamma,\theta_0)$ is the form that $\langle \partial T_\nu/\partial\theta_t\rangle(\theta_t,\theta_0)$ takes when θ_t is expressed in terms of γ and θ_0 through the use of Eqs. (5.11)-(5.14). We consider the cases $\epsilon < 1$ and $\epsilon > 1$ in turn.

$\epsilon < 1$

When $\epsilon < 1$, $\sqrt{\epsilon_2}\cos\theta_t - \sqrt{\epsilon_1}\cos\theta_0$ becomes

$$\sqrt{\epsilon_2}\cos\theta_t - \sqrt{\epsilon_1}\cos\theta_0 = \frac{\sqrt{\epsilon_2}}{1+\gamma^2}[A - \sqrt{\epsilon}(\cos\theta_0 - \gamma\sin\theta_0)] \tag{5.25}$$

with the use of Eq. (5.11). From the definition of A, Eq. (5.14), we find that

$$A > \sqrt{\epsilon}(\cos\theta_0 - \gamma\sin\theta_0). \tag{5.26}$$

As a result we obtain from Eq. (4.4) that

$$s = 1. \tag{5.27}$$

We also obtain the results that

$$\cos(\theta_t - \theta_0) - \sqrt{\epsilon} = \frac{1}{1+\gamma^2}(\cos\theta_0 - \gamma\sin\theta_0)[A - \sqrt{\epsilon}(\cos\theta_0 - \gamma\sin\theta_0)] \tag{5.28}$$

$$\begin{aligned}\sqrt{1/\epsilon} - \cos(\theta_t - \theta_0) &= \frac{1}{1+\gamma^2}\left\{\left(\frac{1}{\sqrt{\epsilon}} - \sqrt{\epsilon}\right)(1+\gamma^2) - (\cos\theta_0 - \gamma\sin\theta_0)\right. \\ &\quad \left.\times[A - \sqrt{\epsilon}(\cos\theta_0 - \gamma\sin\theta_0)]\right\} > 0.\end{aligned} \tag{5.29}$$

If we denote by $t_\nu^{(0)}(\gamma|\theta_0)$ the form $t_\nu^{(0)}(\theta_t|\theta_0)$ takes when θ_t is expressed in terms of γ and θ_0 through the use of Eqs. (5.11)-(5.14), we obtain from the preceding results that

$$t_\nu^{(0)}(\gamma|\theta_0) = \frac{2\sqrt{\epsilon}\mu_\nu}{\cos\theta_t}(\cos\theta_0 - \gamma\sin\theta_0)\tau_\nu^{(0)}(\gamma|\theta_0), \tag{5.30}$$

where

$$\tau_\nu^{(0)}(\gamma|\theta_0) = \frac{(\frac{1}{\sqrt{\epsilon}} - \sqrt{\epsilon})(1+\gamma^2) - (\cos\theta_0 - \gamma\sin\theta_0)[A - \sqrt{\epsilon}(\cos\theta_0 - \gamma\sin\theta_0)]}{\kappa_\nu(\frac{1}{\sqrt{\epsilon}} - \sqrt{\epsilon})(1+\gamma^2) + (\mu_\nu - \kappa_\nu)(\cos\theta_0 - \gamma\sin\theta_0)[A - \sqrt{\epsilon}(\cos\theta_0 - \gamma\sin\theta_0]}. \tag{5.31}$$

The mean differential transmission coefficient, Eq. (5.9), then becomes

$$\left\langle \frac{\partial T_\nu}{\partial\theta_t}\right\rangle(\gamma,\theta_0) = 4\sqrt{\epsilon}\frac{\kappa_\nu\mu_\nu}{\cos\theta_0}(1+\gamma^2)\frac{(\cos\theta_0 - \gamma\sin\theta_0)^2}{[A(\gamma,\theta_0) - \sqrt{\epsilon}(\cos\theta_0 - \gamma\sin\theta_0)]}|\tau_\nu^{(0)}(\gamma|\theta_0)|^2 f(-\gamma). \tag{5.32}$$

We invert this equation and obtain finally

$$f_\nu(\gamma) = \frac{\cos\theta_0}{4\sqrt{\epsilon}\kappa_\nu\mu_\nu}\frac{1}{1+\gamma^2}\frac{[A(-\gamma,\theta_0) - \sqrt{\epsilon}(\cos\theta_0 + \gamma\sin\theta_0)]}{(\cos\theta_0 + \gamma\sin\theta_0)^2}\frac{1}{|\tau_\nu^{(0)}(-\gamma|\theta_0)|^2}\left\langle \frac{\partial T_\nu}{\partial\theta_t}\right\rangle(-\gamma,\theta_0). \tag{5.33}$$

$\epsilon > 1$

When $\epsilon > 1$, $\sqrt{\epsilon_2}\cos\theta_t - \sqrt{\epsilon_1}\cos\theta_0$ is

$$\sqrt{\epsilon_2}\cos\theta_t - \sqrt{\epsilon_1}\cos\theta_0 = -\frac{\sqrt{\epsilon_2}}{1+\gamma^2}[\sqrt{\epsilon}(\cos\theta_0 - \gamma\sin\theta_0) - A]. \tag{5.34}$$

In the present case we find that

$$\sqrt{\epsilon}(\cos\theta_0 - \gamma\sin\theta_0) > A \tag{5.35}$$

as long as $\cos\theta_0 - \gamma\sin\theta_0 > 0$, and γ satisfies either the inequalities (5.21) or (5.22) when $a = 1 - \epsilon\cos^2\theta_0 > 0$, or the inequalities (5.24) when $a = 1 - \epsilon\cos^2\theta_0 < 0$. On the assumption that these conditions are satisfied we obtain from Eq. (4.4) that

$$s = -1. \tag{5.36}$$

We also obtain the results that

$$\sqrt{\epsilon} - \cos(\theta_t - \theta_0) = \frac{1}{1+\gamma^2}(\cos\theta_0 - \gamma\sin\theta_0)[\sqrt{\epsilon}(\cos\theta_0 - \gamma\sin\theta_0) - A] \tag{5.37}$$

$$\begin{aligned}\cos(\theta_t - \theta_0) - \frac{1}{\sqrt{\epsilon}} &= \frac{1}{1+\gamma^2}\left\{\left(\sqrt{\epsilon} - \frac{1}{\sqrt{\epsilon}}\right)(1+\gamma^2) - (\cos\theta_0 - \gamma\sin\theta_0)\right. \\ &\quad \left.\times[\sqrt{\epsilon}(\cos\theta_0 - \gamma\sin\theta_0) - A]\right\}.\end{aligned} \tag{5.38}$$

We can now write $t_\nu^{(0)}(\gamma|\theta_0)$ in the form

$$t_\nu^{(0)}(\gamma|\theta_0) = \frac{2\sqrt{\epsilon}\mu_\nu}{\cos\theta_t}(\cos\theta_0 - \gamma\sin\theta_0)\tau_\nu^{(0)}(\gamma|\theta_0), \tag{5.39}$$

where

$$\begin{aligned}\tau_\nu^{(0)}(\gamma|\theta_0) &= \frac{(\sqrt{\epsilon} - \frac{1}{\sqrt{\epsilon}})(1+\gamma^2) - (\cos\theta_0 - \gamma\sin\theta_0)[\sqrt{\epsilon}(\cos\theta_0 - \gamma\sin\theta_0) - A]}{\kappa_\nu(\sqrt{\epsilon} - \frac{1}{\sqrt{\epsilon}})(1+\gamma^2) + (\mu_\nu - \kappa_\nu)(\cos\theta_0 - \gamma\sin\theta_0)[\sqrt{\epsilon}(\cos\theta_0 - \gamma\sin\theta_0) - A]} \\ &\qquad \text{if} \quad \cos(\theta_t - \theta_0) > \frac{1}{\sqrt{\epsilon}} \qquad (5.40a) \\ &= 0 \qquad \text{if } \cos(\theta_t - \theta_0) < \frac{1}{\sqrt{\epsilon}}. \qquad (5.40b)\end{aligned}$$

The mean differential transmission coefficient now becomes

$$\begin{aligned}\left\langle \frac{\partial T_\nu}{\partial\theta_t} \right\rangle(\gamma, \theta_0) &= 4\sqrt{\epsilon}\kappa_\nu\mu_\nu\frac{1+\gamma^2}{\cos\theta_0}\frac{(\cos\theta_0 - \gamma\sin\theta_0)^2}{\sqrt{\epsilon}(\cos\theta_0 - \gamma\sin\theta_0) - A}|\tau_\nu^{(0)}(\gamma|\theta_0)|^2 f(-\gamma) \\ &\qquad \text{if } \cos(\theta_t - \theta_0) > \frac{1}{\sqrt{\epsilon}} \qquad (5.41a) \\ &= 0 \qquad \text{if } \cos(\theta_t - \theta_0) < \frac{1}{\sqrt{\epsilon}}. \qquad (5.41b)\end{aligned}$$

We invert this result to obtain, finally,

$$f_\nu(\gamma) = \frac{1}{4\sqrt{\epsilon}\kappa_\nu\mu_\nu}\frac{\cos\theta_0}{1+\gamma^2}\frac{\sqrt{\epsilon}(\cos\theta_0+\gamma\sin\theta_0)-A(-\gamma,\theta_0)}{(\cos\theta_0+\gamma\sin\theta_0)^2}\frac{1}{|\tau_\nu^{(0)}(-\gamma|\theta_0)|^2}\left\langle\frac{\partial T_\nu}{\partial\theta_t}\right\rangle(-\gamma,\theta_0). \quad (5.42)$$

6. RESULTS

In this section we apply the results obtained in the preceding section to the determination of the surface profile function in the case where the mean differential transmission coefficient has the form

$$\left\langle\frac{\partial T_\nu}{\partial\theta_t}\right\rangle(\theta_t,\theta_0) = B_\nu\theta(\theta_t-\theta_1)\theta(\theta_2-\theta_t), \quad (6.1)$$

where B_ν is a constant and $\theta(z)$ is the Heaviside unit step function. We assume that

$$\theta_2 = \theta_1 + \Delta\theta, \quad (6.2)$$

where $\Delta\theta$ is a small angular interval, which we take to be 1.5°. Since $\sin\theta$ is a monotonically increasing function of θ in the interval $(-\pi/2,\pi/2)$, we can rewrite Eq. (6.1) as

$$\begin{aligned}\left\langle\frac{\partial T_\nu}{\partial\theta_t}\right\rangle(\theta_t,\theta_0) &= B_\nu\theta(\sin\theta_t-\sin\theta_1)\theta(\sin\theta_2-\sin\theta_t)\\ &= B_\nu\theta(\sqrt{\epsilon}(\sin\theta_0+\gamma\cos\theta_0)-\gamma A(\gamma,\theta_0)-(1+\gamma^2)\sin\theta_1)\\ &\quad\times\theta((1+\gamma^2)\sin\theta_2-\sqrt{\epsilon}(\sin\theta_0+\gamma\cos\theta_0)+\gamma A(\gamma,\theta_0))\\ &= \left\langle\frac{\partial T_\nu}{\partial\theta_t}\right\rangle(\gamma,\theta_0). \quad (6.3)\end{aligned}$$

We have used Eq. (5.12) in obtaining the second form of this expression. The substitution of Eq. (6.3) into Eqs. (5.33) and (5.42) yields the probability density function $f_\nu(\gamma)$ in the case where $\epsilon<1$ and $\epsilon>1$, respectively. The coefficient B_ν is obtained from the normalization of $f_\nu(\gamma)$.

In the usual approach to transmission through a randomly rough surface[1,2] the rejection method[6] is used to generate a long sequence of $\{a_n\}$ from the pdf $f_\nu(\gamma)$, and a realization of the surface profile function $\zeta(x_1)$ is constructed on the basis of Eq. (5.4). The transmission problem is then solved by a rigorous computational approach[7] and the result is used to calculate the differential transmission coefficient on the basis of Eq. (3.11). This process is repeated for N_p realizations of the surface profile function, and an arithmetic average of the N_p results for the differential transmission coefficient yields the mean differential transmission coefficient.

In the present case the form of the mean differential transmission coefficient given by Eqs. (6.1)-(6.2), and the smallness of $\Delta\theta$, have the consequences that such an ensemble average of the differential transmission coefficient is unnecessary. Transmission through a single realization already produces a differential transmission coefficient that is in very good agreement with the result obtained by averaging the results obtained for several hundred realizations of the surface profile function. Consequently in what follows we will mainly present results obtained for only a single realization of the surface profile function.

In Fig. 1 we present results for the case where $\epsilon_1=1$ and $\epsilon_2=2.25$, the incident light is p polarized, its wavelength is $\lambda=632.8$ nm, and the angle of incidence is $\theta_0=15^\circ$. If the interface $x_3=0$ were planar, the angle of transmission, calculated from Snell's law, would be 9.936°. We choose the angle θ_1 to be $\theta_1=-10.686^\circ$, so that $\theta_2=-9.186^\circ$. In Fig. 1(a) we display a short segment of a single realization of the surface profile function calculated for the values of these parameters from Eq. (5.33). The characteristic length b is $b=100\mu$m and

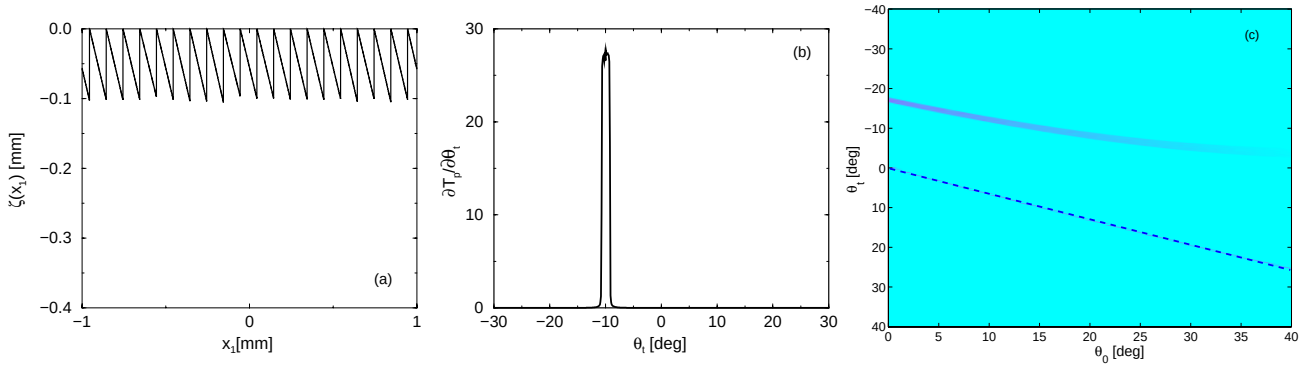

Figure 1. (a) A segment of a single realization of the surface profile function, designed to produce negative refraction of $p-$polarized light incident on it at an angle of incidence $\theta_0 = 15^\circ$; (b) the differential transmission coefficient as a function of the angle of transmission, calculated for this realization of the surface profile function by the use of the Kirchhoff approximation; and (c) a gray level plot of the differential transmission coefficient as a function of the angles of incidence and transmission.

the value of N entering Eq. (5.4) is $N = 1000$ ($L_1 = 20$ cm). In Fig. 1(b) we present a plot of the differential transmission coefficient as a function of the angle of transmission, calculated for this realization of the surface profile function by the Kirchhoff approximation,[8] due to its simplicity and speed. It is seen to consist of a single narrow peak of width 1.5°, centered at $\theta_t = -9.936^\circ$. Thus, for this angle of incidence the light transmitted through the random interface undergoes negative refraction. As the angle of incidence is moved away from 15°, while the surface remains fixed, the angular position of this peak also moves. In Fig. 1(c) we present a gray-level plot of the differential transmission coefficient as a function of the angles of incidence and transmission. The large values of the differential transmission coefficient in Fig. 1(c) trace the dependence of the angle of refraction θ_t on the angle of incidence θ_0, for θ_0 in the vicinity of 15°. The dashed line also plotted in this figure is the dependence $\theta_t = \sin^{-1}(\sqrt{\epsilon_1/e_2}\sin\theta_0)$ of the transmission angle on the incidence angle in the case that the interface $x_3 = 0$ is planar. It is seen that for the surface profile chosen the transmitted light undergoes nonstandard refraction, including negative refraction, over a wide range of angles of incidence.

In Fig. 2 we present the analogous results for the same values of the material and experimental parameters assumed in obtaining Fig. 1, but for the case where the incident light is s polarized. The results are qualitatively and quantitatively similar to those obtained when the incident light is p polarized. The differential transmission coefficient at its maximum is slightly higher in the case of $p-$polarized light due to its weaker reflection from the facets forming the surface.

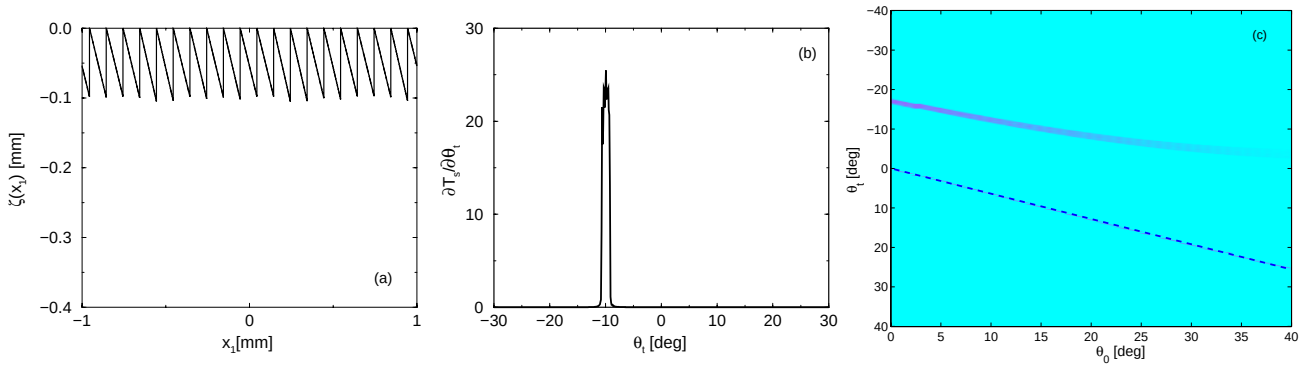

Figure 2: The same as in Fig. 1 but for $s-$polarized incident light.

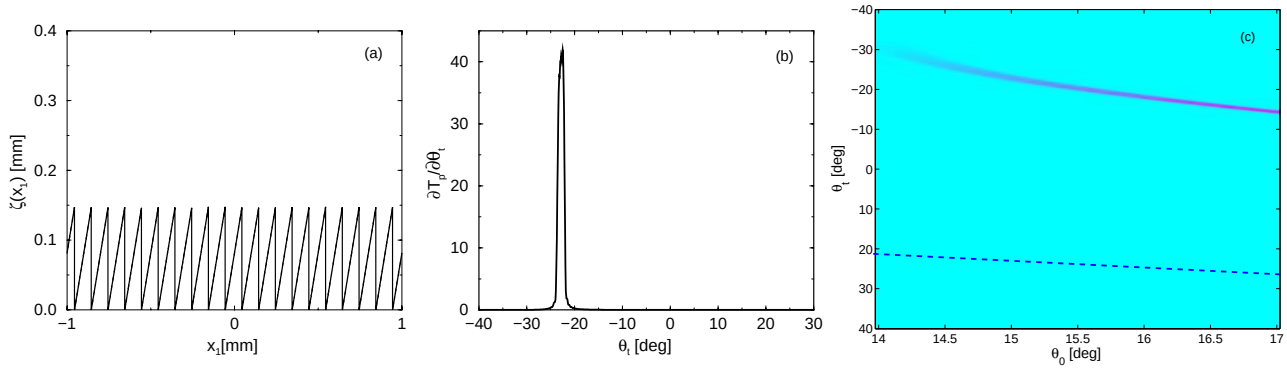

Figure 3. (a) A segment of a single realization of the surface profile function, designed to produce negative refraction of $p-$polarized light incident on it at an angle of incidence $\theta_0 = 15^\circ$; (b) the differential transmission coefficient as a function of the angle of transmission, calculated for this realization of the surface profile function by the use of the Kirchhoff approximation; and (c) a gray level plot of the differential transmission coefficient as a function of the angles of incidence and transmission.

We turn now to the case where the medium of incidence is the optically more dense medium, and present results in Fig. 3 for the case where $\epsilon_1 = 2.25$, $\epsilon_2 = 1$, the incident light is p polarized, its wavelength is $\lambda = 632.8$ nm, and the angle of incidence is $\theta_0 = 15^\circ$. In the case that the interface $x_3 = 0$ is planar, there is a critical angle for total internal reflection, $\theta_c = \sin^{-1}\sqrt{\epsilon_2/\epsilon_1} = 41.81^\circ$, while the angle of transmission obtained from Snell's law is 22.844°. We choose the angle θ_1 to be $\theta_1 = -23.594^\circ$, so that $\theta_2 = -22.094^\circ$. In Fig. 3(a) we plot a segment of one realization of the surface profile function calculated for these values of the parameters from Eq. (5.42) with $b = 100\mu$m and $N = 1000$. In Fig. 3(b) the differential transmission coefficient, calculated for this surface profile function by the Kirchhoff approximation[8] is plotted as a function of the angle of transmission. It consists of a single narrow peak of width 1.5° centered at $\theta_t = -22.844^\circ$. The surface we have designed therefore negatively refracts light incident on it at an angle $\theta_0 = 15^\circ$. In Fig. 3(c) we present a gray level plot of the differential transmission coefficient as a function of the angles of incidence and transmission for this surface profile function for a range of values of θ_0 in the vicinity of $\theta_0 = 15^\circ$. The dashed line also plotted in this figure is the dependence $\theta_t = \sin^{-1}(\sqrt{\epsilon_1/e_2}\sin\theta_0)$ of the transmission angle on the incidence angle when the interface $x_3 = 0$ is planar, and we see that the transmitted light undergoes nonstandard refraction, including negative refraction, over a large range of values of the angle of incidence.

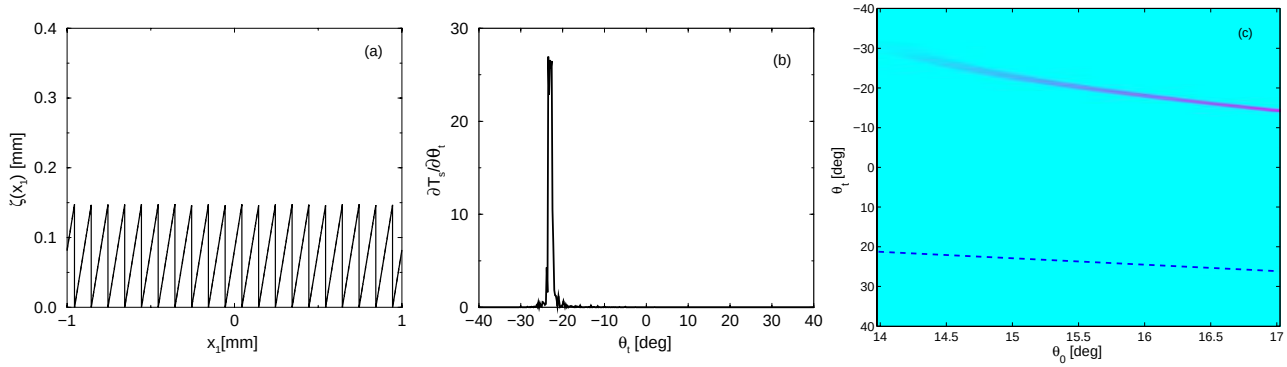

Figure 4: The same as in Fig. 3 but for $s-$polarized incident light.

Finally, in Fig. 4 we present the analogous results for the same values of the material and experimental parameters assumed in obtaining Fig. 3, except that the incident light is now s polarized. As in the case of the results presented in Figs. 1 and 2, the results presented in Fig. 4 are qualitatively similar to those presented

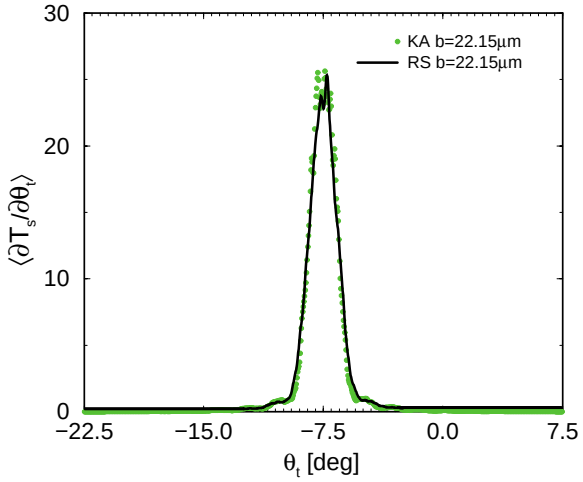

Figure 5. The differential transmission coefficient for $s-$polarized light incident at an angle $\theta_0 = 5^\circ$ as a function of the angle of transmission, calculated by the use of the rigorous simulations (RS) (thick line) and the Kirchhoff approximation (KA) (circles). The characteristic length b is $b = 35\lambda \approx 22.15\mu$m and $N = 3$ ($L_1 = 130\mu$m).

in Fig. 3, but are quantitatively different. In this case the differential transmission coefficient at its maximum is considerably higher in the case of $p-$polarized light. This is because the local angles of incidence are close to the Brewster angle, so that the reflection from each of the facets forming the surface is considerably weaker than it is for $s-$polarized light.

As we have noted above, the results plotted in Figs. 1-4 were calculated by the use of the Kirchhoff approximation, due to its simplicity and speed. However, this approximation does not take into account the vertical segments of the surface profile function nor potential multiple-scattering effects. To see how this neglect influences the results obtained we have also solved the scattering problem by a rigorous approach based on Green's second integral identity in the plane[4] in which the scattering from these segments is fully taken into account.[9] In Fig. 5 the thick solid black line represents the result of the rigorous numerical simulations for the case where $\epsilon_1 = 2.25$ and $\epsilon_2 = 1$, the incident light is s polarized, its wavelength is $\lambda = 632.8$ nm, and the angle of incidence is $\theta_0 = 5^\circ$. In this case the angle of transmission obtained from Snell's law is 7.512°, the angle θ_1 is $\theta_1 = -8.262^\circ$, so that $\theta_2 = -6.762^\circ$. The characteristic length b is $b = 35\lambda \approx 22.15\mu$m, and the value of N entering Eq. (5.4) is $N = 3$ ($L_1 = 130\mu$m). Since the short surfaces generated with such small values of N cannot fully possess the statistics of an infinitely long random surface, averaging over the ensemble of realizations of the surface was needed in this case. Thus, the curve represented by the thick solid black line in Fig. 5 is an arithmetic average of the results obtained for $N_p = 250$ realizations of the random surface. For comparison the circles show the result obtained by the use of the Kirchhoff approximation for the same values of the parameters, and is also an average over results obtained for $N_p = 250$ realizations of the surface profile function. The results presented in Fig. 5 shows that the use of the Kirchhoff approximation produces quantitatively good results.

7. DISCUSSION

On the basis of the geometrical optics limit of the Kirchhoff approximation we have developed an approach to the design of a one-dimensional randomly rough interface between two different dielectric media that produces a transmitted field with a specified dependence of the mean differential transmission coefficient on the angle of transmission for any specified angle of incidence. We have applied this method to the case where the mean differential transmission coefficient as a function of the angle of transmission has a constant value within a

very narrow angular interval, centered at the negative of the angle of transmission given by Snell's law when the interface between the two media is planar, and vanishes outside this interval. The light incident on the interface in this case undergoes a form of negative refraction. Although the interface was designed on the basis of a single-scattering approximation, calculations of the mean differential reflection coefficient by means of a rigorous numerical approach that takes multiple-scattering processes of all orders into account show that the interface designed in this way transmits light in the manner it was designed to do.

For the same interfaces we have also investigated the dependence of the angle of transmission on the angle of incidence, when the latter is in the vicinity of the value for which the interface was designed. This dependence shows that the interface refracts light negatively for a large range of values of the angle of incidence.

These properties of the interfaces designed here are consequences of their roughness alone, and do not require the presence of any negative index material. These interfaces could be used in applications requiring negative refraction.[10]

Finally, we note that interfaces of this type can be fabricated at the interface between air and photoresist by the method described in.[8]

Acknowledgements

The research of TAL and AAM was supported in part by AFRL contract FA9453-08-C-0230. The research of IS was supported in part by AFRL contract FA9453-08-C-0230 and The Research Council of Norway Småforsk (Project no. 10330600).

REFERENCES

1. T. A. Leskova, A. A. Maradudin, E. R. Méndez, and I. Simonsen, "A band-limited uniform diffuser in transmission," SPIE **4100**, 113-123 (2000).
2. A. A. Maradudin, E R. Méndez, T. A. Leskova, and I. Simonsen, "A band limited uniform diffuser in transmission. II. A multilayer system," SPIE **4447**, 130-139 (2001).
3. V. G. Veselago, "The electrodynamics of substances with simultaneously negative values of ϵ and μ," Sov. Phys. Usp. **10**, 509-514 (1968).
4. A. E. Danese, *Advanced Calculus*, vol. I (Allyn and Bacon, Boston, 1965), p. 123.
5. A. G. Voronovich, "The Kirchhoff and related approximations," in *Light Scattering and Nanoscale Surface Roughness*," ed. A. A. Maradudin (Springer, New York, 2006), pp. 35-60.
6. W. H. Press, S. A. Teukolsky, W. T. Vetterling, and B. P. Flannery, *Numerical Recipes in Fortran*, second ed. (Cambridge University Press, New York, 1992), pp. 281-282.
7. A. A. Maradudin, T. Michel, A. R. McGurn, and E. R. Méndez, "Enhanced backscattering of light from a random grating," Ann. Phys. (N.Y.) **203**, 255-307 (1990).
8. E. R. Méndez, E. E. García-Guerrero, T. A. Leskova, A. A. Maradudin, J. Muñoz-Lopez, and I. Simonsen, "The design of one-dimensional random surfaces with specified scattering properties," Appl. Phys. Lett. **81**, 798-800 (2002).
9. A. A. Maradudin, E. R. Méndez, and T. A. Leskova, *Designer Surfaces* (Elsevier, Amsterdam, 2008) pp. 111-118.
10. See, for example, W. T. Lu, Y. J. Huang, P. Vodo, R. K. Banyal, C. H. Perry, and S. Sridhar, "A new mechanism for negative refraction and focusing using selective diffraction from surface corrugation," Opt. Express **15**, 9166-9175 (2007).